

Magnetic properties of GaMnAs from an effective Heisenberg Hamiltonian

L. Brey¹ and G. Gómez-Santos²¹*Instituto de Ciencia de Materiales de Madrid (CSIC), Cantoblanco, 28049 Madrid, Spain*²*Departamento de Física de la Materia Condensada and Instituto Nicolás Cabrera, Universidad Autónoma de Madrid, 28049 Madrid, Spain*

(Received 5 June 2003; revised manuscript received 24 July 2003; published 26 September 2003)

We introduce a Heisenberg Hamiltonian for describing the magnetic properties of GaMnAs. Electronic degrees of freedom are integrated, leading to a pairwise interaction between Mn spins. Monte Carlo simulations in large systems are then possible, and reliable values for the Curie temperatures of diluted magnetic semiconductors can be obtained. Comparison of mean field and Monte Carlo Curie temperatures shows that fluctuation effects are important for systems with a large hole density and/or increasing locality in the carriers-Mn coupling. We have also compared the results obtained by using a realistic $\mathbf{k} \cdot \mathbf{p}$ model with those of a simplified parabolic two band model. In the two-band model, the existence of a spherical Fermi surface produces the expected sign oscillations in the coupling between Mn spins, magnifying the effect of fluctuations and leading to the eventual disappearance of ferromagnetism. In the more realistic $\mathbf{k} \cdot \mathbf{p}$ model, warping of the Fermi surface diminishes the sign oscillations in the effective coupling and, therefore, the effect of fluctuations on the critical temperature is severely reduced. Finally, by studying the collective magnetic excitations of this model at zero temperature, we analyze the stability of the fully polarized ferromagnetic ground state.

DOI: 10.1103/PhysRevB.68.115206

PACS number(s): 75.50.Pp, 75.10.-b

I. INTRODUCTION

In recent years, one of the most studied diluted magnetic semiconductor (DMS) has been $\text{Ga}_{1-x}\text{Mn}_x\text{As}$.¹⁻³ Ideally, the Mn ions substitute Ga atoms, close a d shell acquiring a core spin $S=5/2$, and give a hole to the system. Due to the experimental growth conditions, these semiconductors have defects in the positions of Ga and As atoms (antisite defects), and in the location of Mn ions (interstitials). Some of these defects act as donors that partially compensate the holes contributed by the Mn ions.³ Therefore, the density of holes, p , is generally smaller than the density of Mn ions, c .

Experimentally, high Curie temperatures (T_C) are observed near an optimal doping around $x \sim 0.05$. At these dilute concentrations, direct interaction between Mn ions can be neglected. However, Mn spins have a strong antiferromagnetic kinetic exchange coupling J_{pd} with hole spins.⁴ For metallic systems, the motion of holes mediates a ferromagnetic interaction between the Mn ions, leading to spontaneous magnetization with experimental T_C as high as 160 K.⁵

A first approach to the problem consists in describing the electronic system within the virtual-crystal approximation, and the thermal effects in the mean-field approximation.^{6,7} In this scheme, the hole spins feel the magnetic field created by the Mn spins which, in turn, are equally affected by the effective field of hole spins. Therefore, Mn ions and holes become coupled by J_{pd} , and the low-temperature phase exhibits ferromagnetism with Curie temperature:

$$k_B T_C^{vca} = \frac{S^2 J_{pd}^2}{3} \chi_p(q=0)c, \quad (1)$$

where $\chi_p(q=0)$ is the zero wave-vector paramagnetic susceptibility of the hole gas.⁸ This expression indicates that the Curie temperature can be increased by raising the density of Mn ions and/or the number of holes. The former possibility

is limited by the tendency of the Mn ions to form clusters of antiferromagnetically coupled Mn spins, which do not contribute mobile holes to the host semiconductor. The latter possibility has been explored experimentally by different groups.^{5,9,10} They have performed annealing treatments to molecular-beam epitaxy grown GaMnAs samples. In this process, the number of defects acting as donors is reduced and, therefore, the number of holes increases. In this way, the Curie temperature has been raised from 60 K to 160 K,⁵ for a Mn concentration of $x=0.08$.

The natural question that arises concerns the possibility of further increasing Curie temperatures. Experimental studies of the Mn ferromagnetic moment in postannealed samples show that a large fraction of Mn spins (more than 50%) do not participate in the ferromagnetism.⁹ This result opens up the possibility of increasing Curie temperatures by a better alignment of the Mn spins in the zero-temperature ground state of the system. Therefore, it is very important to know whether the observed lack of magnetization saturation is due to an extrinsic effect such as the *wrong* location of some Mn ions in the host semiconductor, or rather due to intrinsic frustration related to the spatial oscillatory behavior of the hole mediated interaction between Mn spins. The study of this last possibility provides the main motivation for this work.

As already mentioned, usual mean-field calculations like that of Eq. (1) (Ref. 6,7) assume a virtual-crystal approximation (VCA), where the Mn ions are replaced by a uniform magnetic field acting on the hole spins. This approach does not describe the individual interactions between the Mn spins and the holes, and always predicts a fully saturated ferromagnetic ground state (GS) for the Mn spins. There have been several attempts to study the effect that thermal fluctuations and disorder have on the value of T_C ,¹¹⁻¹⁴ by means of Monte Carlo (MC) simulations. By disorder we mean the random location of the Mn ions on the fcc lattice of the host semiconductor. These calculations have strong finite-size ef-

fects because, even though the Mn spins are treated classically, the carriers kinetic energy must be evaluated at each MC step, requiring the diagonalization of the electron Hamiltonian. Therefore, MC simulations have been limited to simple electronic models (one-orbital tight-binding Hamiltonian or two-band parabolic model) and to small systems (less than 600 Mn ions and 60 carriers).

On the other hand, Schliemann and MacDonald^{15,16} have studied the effect that disorder and quantum fluctuations have on the zero-temperature GS, using perturbation theory and a two-band model. They conclude that long-range fluctuations make the full ferromagnetic phase unstable against a noncollinear ferromagnetic state. In the same direction and using a four-band model, Zaránd and Jankó¹⁷ have obtained that, due to the large spin-orbit coupling existing in the host semiconductor, the interaction between Mn spins is highly anisotropic, concluding that the zero temperature GS is intrinsically spin disordered. Also recently, using a disordered Ruderman-Kittel-Kasuya-Yosida (RKKY) lattice mean-field theory for a two-band model, Priour *et al.*¹⁸ mention that the presence of direct af coupling between magnetic impurities can lead to unsaturated polarization of the Mn ions.

In this work we study the effect that disorder and thermal fluctuations have on the value of T_C . We also analyze the effect that disorder and quantum fluctuations have on the zero-temperature GS of the system. To this end, we introduce a Heisenberg-like Hamiltonian with pairwise interactions between Mn ions for describing the magnetic properties of GaMnAs. This approach just requires the position and spin orientation of the Mn ions, without explicit consideration of the electronic degrees of freedom. To be precise, we propose the following functional:

$$E = E_{KE} - \sum_{I,J} J(\mathbf{R}_{IJ}) \mathbf{S}_I \cdot \mathbf{S}_J, \quad (2)$$

where the coupling constant $J(\mathbf{R}_{IJ})$ is obtained using a realistic six-band $\mathbf{k} \cdot \mathbf{p}$ Hamiltonian. The indices (I, J) run on the position of the Mn spins, which are randomly located at sites \mathbf{R}_I of the host semiconductor fcc lattice, with $\mathbf{R}_{IJ} = \mathbf{R}_I - \mathbf{R}_J$. We will justify the correctness of this procedure for the expected range of parameters and, furthermore, show that $J(\mathbf{R}_{IJ})$ can be obtained perturbatively. As the electronic degrees of freedom are integrated inside these coupling constants, we can perform large MC simulations for estimating the value of T_C . Also, treating Mn spins as quantum objects, we will be able to study collective magnetic excitations of Eq. (2) and analyze the stability of the zero-temperature ferromagnetic GS. This will be done by means of an explicit calculation of coupling constants $J(\mathbf{R}_{IJ})$ in the spin-polarized background of carriers at zero temperature.

The paper is organized as follows. Section II presents the microscopic model. In Sec. III, we deduce the Hamiltonian of Eq. (2) from the microscopic model and justify its use. In Sec. IV, the coupling constants of the pairwise Hamiltonian are obtained perturbatively, and mean-field treatments are revised. A criterion is introduced to quantitatively assess the effect of fluctuations from the mere analysis of interactions. Results of MC are shown in Sec. V for both the two-band

and six-band models. The importance of fluctuations (thermal and disorder), their dependence on system parameters, and their impact on the critical temperature are particularly considered. In Sec. VI, we study our model in the zero-temperature limit. We obtain the density of states of collective magnetic excitations and analyze the stability of the zero-temperature ferromagnetic ground state. In Sec. VII we conclude the paper with the conclusions.

II. THE MICROSCOPIC MODEL

As explained above, we assume that Mn ions, with a $3d^5$ and $S=5/2$ configuration, are randomly located in a fcc lattice. These ions donate a density p of holes to the system that, according to photoemission studies,¹⁹ have a strong $4p$ character that should be associated with valence-band states of the host semiconductor. Therefore, we model the motion of holes in the host semiconductor and their interaction with the Mn spins with the following Hamiltonian:

$$H = H_{holes} + \sum_I \int d^3\mathbf{r} \mathbf{s}(\mathbf{r}) \cdot \mathbf{S}_I \tilde{J}(\mathbf{r} - \mathbf{R}_I), \quad (3)$$

where $\mathbf{s}(\mathbf{r})$ is the spin density of carriers antiferromagnetically coupled to the Mn spins \mathbf{S}_I located at random positions \mathbf{R}_I of the fcc lattice. The exchange coupling $\tilde{J}(\mathbf{r})$ has a spatial extension that we model as a Gaussian of width a_0 :

$$\tilde{J}(\mathbf{r}) = \frac{J_{pd}}{(2\pi a_0^2)^{3/2}} e^{-r^2/2a_0^2}. \quad (4)$$

J_{pd} parametrizes the strength of the coupling, whereas the parameter a_0 is a measure of the nonlocal character of this interaction. a_0 should be of the order of the first neighbors distance, which corresponds to the minimum separation between the Mn- d orbitals and the GaAs- p orbitals that form the hole bands of the host semiconductor. Experimental work¹⁹ estimates $J_{pd} \approx 60$ meV nm³. As the Mn ions are rather diluted, we have neglected any direct superexchange interaction between them. The term H_{holes} , representing the motion of holes in the semiconductor, is described with a realistic six-band $\mathbf{k} \cdot \mathbf{p}$ envelope function formalism.²⁰ In the actual magnetic semiconductors, the carrier density is of the order of 10^{20} cm⁻³ and, for these values, it seems justified to neglect the effect of the carrier-carrier interaction. As we know²¹ that the rearrangement of defects considerably weakens the interaction between carriers and defects, we also neglect any effect of disorder in the motion of carriers beyond the mere magnetic coupling of Eq. (3).

In the $\mathbf{k} \cdot \mathbf{p}$ model,²² the hole wave functions are described by a band index n and a wave vector \mathbf{k} , having the form

$$\psi_{n,\mathbf{k}}(\mathbf{r}) = e^{i\mathbf{k}\mathbf{r}} \sum_{J,m_J} \alpha_{n,\mathbf{k}}^{J,m_J} u_{J,m_J}(\mathbf{r}), \quad (5)$$

$$u_{J,m_J}(\mathbf{r}) = \frac{1}{\sqrt{N}} \sum_I \phi_{J,m_J}(\mathbf{r} - \mathbf{R}_I), \quad (6)$$

where $u_{J,m_J}(\mathbf{r})$ are the six Γ_{4v} valence-band wave functions with $k=0$ and ϕ_{J,m_J} represent atomiclike orbitals with total angular momentum J , and z component of the angular momentum m_J . The six higher-energy valence-band states of GaAs correspond to $J=3/2$ and $J=1/2$. In Eq. (6), the index I runs over all the (N) sites of the fcc lattice, and \sqrt{N} is the normalization factor. The parameters that determine the wave functions $\alpha_{n,\mathbf{k}}^{J,m_J}$ and the corresponding eigenvalues $\epsilon_{n,\mathbf{k}}$ are obtained by diagonalizing a 6×6 matrix²² for each wave vector. The entries of this matrix depend on the spin-orbit coupling Δ_{so} , the Kohn-Luttinger parameters γ_i , and on the wave vector \mathbf{k} . We use parameters appropriated for GaAs,²² with values $\gamma_1=6.85$, $\gamma_2=2.1$, $\gamma_3=2.9$, and $\Delta_{so}=0.34$ eV.

In the $\mathbf{k} \cdot \mathbf{p}$ basis, the Hamiltonian of Eq. (3) has the form

$$H = \sum_{n\mathbf{k}} \epsilon_{n\mathbf{k}} c_{n\mathbf{k}}^\dagger c_{n\mathbf{k}} + \sum_{n\mathbf{k}, n'\mathbf{k}'} \langle n\mathbf{k} | V | n'\mathbf{k}' \rangle c_{n\mathbf{k}}^\dagger c_{n'\mathbf{k}'}, \quad (7)$$

where $c_{n\mathbf{k}}^\dagger$ creates a hole with quantum numbers n and \mathbf{k} . The second term of this equation is the interaction between the holes and the Mn spins:

$$\begin{aligned} \langle n\mathbf{k} | V | n'\mathbf{k}' \rangle &= \frac{J_{pd}}{\Omega} \sum_I e^{-i(\mathbf{k}-\mathbf{k}')\mathbf{R}_I} \mathbf{S}_I \cdot \langle n', \mathbf{k}' | \mathbf{s} | n, \mathbf{k} \rangle \\ &\times e^{-(\mathbf{k}-\mathbf{k}')^2 a_0^2/2}, \end{aligned} \quad (8)$$

where

$$\langle n', \mathbf{k}' | \mathbf{s} | n, \mathbf{k} \rangle = \sum_{Jm_J, J'm_J'} (\alpha_{n,\mathbf{k}}^{J,m_J})^* \alpha_{n',\mathbf{k}'}^{J',m_J'} \mathbf{s}_{Jm_J, J'm_J'},$$

the index I runs over Mn locations, $\mathbf{s}_{Jm_J, J'm_J'}$ is the matrix element of the hole spin operator in the local angular momentum basis,²⁰ and Ω is the system volume. The eigenenergies of this Hamiltonian can be written in the form

$$E = E_{KE} + \Delta E, \quad (9)$$

E_{KE} being the energy of the carriers in absence of exchange coupling with the Mn ions and ΔE the variation of the system energy due to the hole-Mn spin interaction. We take E_{KE} as our zero of energy.

III. PAIRWISE INTERACTIONS BETWEEN MANGANESE SPINS

In this section we will justify the validity of the Heisenberg-like model of Eq. (2) for the experimentally relevant range of parameters, with coupling constants $J(\mathbf{R}_{IJ})$ obtained perturbatively.

A. Interaction energy of a pair of Mn spins: Spin and spatial anisotropies

Our first result is that the interaction between two Mn spins \mathbf{S}_1 and \mathbf{S}_2 is very well described by their scalar product. To show this, we have calculated the energy of a system containing just two Mn ions: one located at the origin with

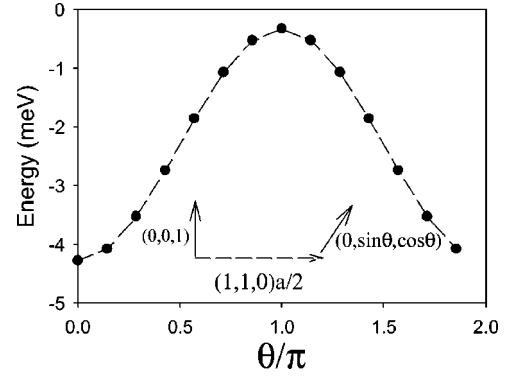


FIG. 1. Energy of a system formed by two Mn ions. One is located at $(0,0,0)$, with its spin pointing in the $(0,0,1)$ direction, the other is at $(0,1,1)a/2$, with its spin oriented in the $(0, \sin \theta, \cos \theta)$ direction. The calculations have been done for a hole density $p = 0.44 \text{ nm}^{-3}$, a coupling $J_{pd} = 0.06 \text{ eV nm}^3$, and a spatial extension of the interaction $a_0 = 4 \text{ \AA}$.

its spin pointing in the $(0,0,1)$ direction and the other placed at one of the first neighbor positions $(0,a,a)/2$ of the fcc lattice ($a = 5.66 \text{ \AA}$ for GaAs) with its spin pointing in the $(0, \sin \theta, \cos \theta)$ direction. In Fig. 1 we plot this energy for different relative orientations θ for a hole density $p = 0.44 \text{ nm}^{-3}$, an exchange-coupling $J_{pd} = 0.06 \text{ eV nm}^3$, and a spatial extension of the coupling $a_0 = 4 \text{ \AA}$. We see that the interaction energy can be fitted very well by $\cos \theta$. Since we expect spin anisotropies to show up predominantly at short distances, its absence for nearest neighbors makes us conclude that a spin isotropic interaction is appropriate for arbitrarily separated Mn spins. Therefore, we write the energy of a pair of Mn spins \mathbf{S}_1 and \mathbf{S}_2 , separated by an arbitrary vector $(i,j,k)a/2$, in the form

$$\Delta E = 2\Sigma + \Delta U_{i,j,k} \frac{\mathbf{S}_1 \cdot \mathbf{S}_2}{S^2}, \quad (10)$$

with

$$\Delta U_{ijk} = \frac{1}{2} [\Delta_{ijk}^{(2)}(\uparrow, \uparrow) - \Delta_{ijk}^{(2)}(\uparrow, \downarrow)],$$

$$\Sigma = \frac{1}{4} [\Delta_{ijk}^{(2)}(\uparrow, \uparrow) + \Delta_{ijk}^{(2)}(\uparrow, \downarrow)], \quad (11)$$

where the expressions $\Delta_{ijk}^{(2)}(\uparrow, \uparrow)$ and $\Delta_{ijk}^{(2)}(\uparrow, \downarrow)$ represent the energies of a pair of Mn spins separated by a vector $(i,j,k)a/2$, with parallel and antiparallel spins in the z direction. Σ is a self-interaction energy that neither depends on (i,j,k) nor affects the spin coupling.

Recently, Zaránd and Jankó¹⁷ derived that the Mn-Mn interaction in GaMnAs is highly anisotropic, using a four-band model.²³ This anisotropy is due to the p character of the top valence bands and the large spin-orbit coupling existing in GaAs. In particular, they found that the interaction between two parallel spins separated by a vector \mathbf{R} is different depending on whether the spins point along the vector \mathbf{R} or perpendicular to it. This large anisotropy predicted in Ref. 17 seems to be in contradiction with the results presented in Fig. 1, where a simple cosine fits the interaction very well. In order to study the spin anisotropy more carefully, we have

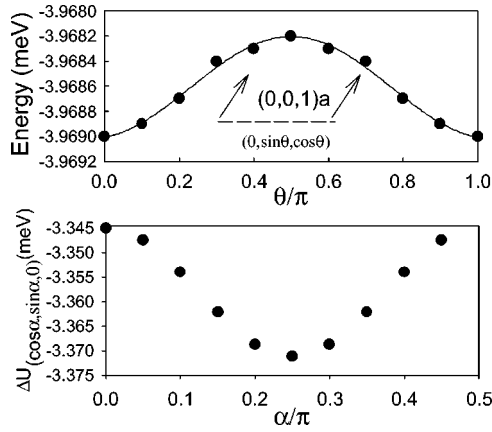


FIG. 2. Top panel: Energy of a system formed by two Mn ions located at $(0,0,0)$ and at $(0,0,a)$. Mn spins are parallel and point in the $(0,\sin\theta,\cos\theta)$ direction. The calculations have been done for $p=0.44 \text{ nm}^{-3}$, $J_{pd}=0.06 \text{ eV nm}^3$, and $a_0=4 \text{ \AA}$. Bottom panel: Interaction energy of a system formed by two Mn ions located at $(0,0,0)$ and at $(\cos\alpha,\sin\alpha,0)a$, for the same parameters. Mn spins point in the z direction.

calculated the energy of a pair of parallel Mn spins pointing in the $(0,\sin\theta,\cos\theta)$ direction and separated by a vector $(0,0,a)$. In Fig. 2 (top panel), we plot the energy of this configuration as a function of θ . We obtain, in agreement with Ref. 17, that the interaction energy depends on the angle formed by the spins and the vector joining them. Quantitatively, however, this anisotropy is very small: less than 10^{-4} times smaller than the interaction energy and, therefore, it can be safely neglected. We have found that this spin anisotropy becomes larger for smaller values of the spatial extension of the interaction a_0 , but always remains smaller than 5% of the interaction energy, even for the extreme case of a purely local coupling $a_0=0$. We have checked that the discrepancy between the results of Zaránd and Jankó and ours originates in the different models used for the band structure. The four-band chiral spherical model used in Ref. 17 considers an infinite spin-orbit coupling and, therefore, overestimates considerably the spin anisotropy of the interaction.

Due to the p character of the higher-energy valence-band states of GaAs, the symmetry of the $\mathbf{k}\cdot\mathbf{p}$ Hamiltonian is cubic. Therefore, spatial directions not related by the symmetry operations of the cubic group are not equivalent. In order to estimate this spatial anisotropy, we have calculated the exchange interaction energy, Eq. (11), for two Mn ions located at $(0,0,0)$ and at $(\cos\alpha,\sin\alpha,0)a$, and with spins oriented in the z direction. Using this geometry, we avoid the effects associated with the spin anisotropy discussed before, leaving alone the spatial anisotropy. In Fig. 2 (bottom panel) we plot the interaction energy as a function of the angle α . We observe that the interaction energy depends very weakly on the orientation of the vector that joins the Mn spins. As in the case of spin anisotropy, the effect of the spatial anisotropy is also larger for smaller values of a_0 , but always remains smaller than 5%. In conclusion, an expression such as Eq. (2), with a coupling constant dependent on distance but not on orientation, provides an adequate description for the interaction between two Mn spins.

B. Virial expansion and perturbation theory

Previous MC simulations¹³ have shown that the Curie temperature of DMS increases linearly with x for low Mn concentration. This linearity strongly suggests that a virial-like approach, where the Mn interaction is expressed as a sum of pairwise terms, should provide a good approximation in this low-concentration regime.

In order to test the validity of this approach, we have computed the energy of a three Mn ions system, comparing the result with the energy of three systems containing only two Mn ions. We place three Mn ions at close positions $(0,0,0)$, $(1,0,0)a$, and $(0,1,0)a$, and call $\Delta^{(3)}$ the exact energy of this three-body system. Assuming only pairwise interactions, the energy to be associated to this system can be written as [see Eq. (11)]

$$\Delta_{pairs}^{(3)} = 3\Sigma + \Delta U_{020} + \Delta U_{200} + \Delta U_{220}. \quad (12)$$

The comparison between the exact and pairwise approximated energies for the parameters $p=0.44 \text{ nm}^{-3}$, $J_{pd}=0.06 \text{ eV nm}^3$, and $a_0=4 \text{ \AA}$, provides the following results:

$$\Delta^{(3)} = -5.043 \text{ meV}, \quad \Delta_{pair}^{(3)} = -5.031 \text{ meV}. \quad (13)$$

From these numbers we conclude that writing the energy of the system as a sum of pair interactions is indeed a very good approximation for DMS.

The interaction energies presented in the preceding sections were obtained by solving the Hamiltonian (3). From these calculations we have justified the use of a Heisenberg-like Hamiltonian for describing the magnetic properties of GaMnAs. In this approach, the coupling constants $J(\mathbf{R}_{IJ})$ have been obtained by solving Eq. (3) for different distances between Mn ions, and for parallel and antiparallel orientation of their spins. The exact solution of the Hamiltonian (3), even for only two Mn ions as in the preceding sections, requires the diagonalization of very large complex matrices (larger than 3000×3000), posing a severe computational problem.

To bypass this difficulty, we have resorted to perturbation theory for the calculation of coupling constants. We know that, for small values of the exchange coupling, a second-order perturbation theory treatment of V [Eq. (8)] should be valid, leading to interaction energies proportional to J_{pd}^2 . In order to check the validity of a perturbative treatment, we have calculated the interaction energy of a system formed by two Mn spins located at positions $(0,0,0)$ and $(1,1,0)a/2$, for the parameters $p=0.44 \text{ nm}^{-3}$ and $a_0=4 \text{ \AA}$. The results, plotted in Fig. 3, confirm that the interaction energy remains quadratic until values of the exchange coupling of the order $J_{pd} \sim 100 \text{ meV nm}^3$. It is worth mentioning here that although previous MC simulations^{11,13} have found deviations from the quadratic dependence of the Curie temperature on J_{pd} , these deviations appear at values of J_{pd} larger than 0.1 eV nm^{-3} . Therefore, we conclude that the use of perturbation theory for computing the interaction energies is appropriated for the expected range of parameters, enormously simplifying the computational effort.

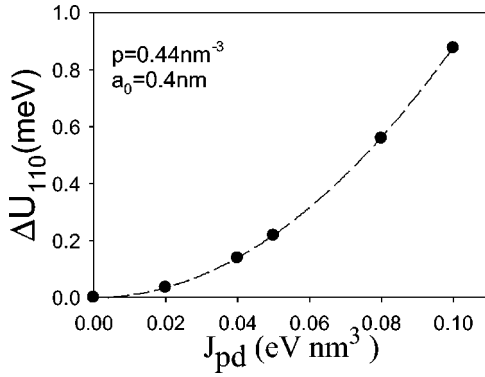


FIG. 3. Interaction energy as function of J_{pd} of a system formed by two Mn ions located at (0,0,0) and at (1,1,0) $a/2$.

It is interesting to note that the perturbative regime, with its associated small values of coupling constants, fits nicely within the virial expansion approach. Three-body interactions will only appear to order J_{pd}^3 , making us expect our pair interaction approximation to be valid even for not so low impurity concentrations, provided the coupling constant remains small.

IV. HEISENBERG HAMILTONIAN: MEAN-FIELD TREATMENTS AND FLUCTUATIONS

The calculations presented in the preceding section justify the description of magnetic properties of GaMnAs in terms of a two-body, spin isotropic, Heisenberg-like Hamiltonian:

$$H = - \sum_{I,J} J(\mathbf{R}_{IJ}) \mathbf{S}_I \cdot \mathbf{S}_J, \quad (14)$$

with exchange coupling given by

$$J(\mathbf{R}_{IJ}) = \frac{1}{N} \sum_{\mathbf{q}} j(\mathbf{q}) e^{i\mathbf{q}\mathbf{R}_{IJ}}. \quad (15)$$

The Fourier-transformed coupling $j(\mathbf{q})$ is given by

$$j(\mathbf{q}) = J_{pd}^2 \frac{N}{\Omega} \chi_p(\mathbf{q}) e^{-q^2 a_0^2}, \quad (16)$$

with the paramagnetic susceptibility obtained in the standard perturbative manner from the original Hamiltonian of Eq. (3):

$$\chi(\mathbf{q}) = \frac{1}{\Omega} \sum_{n',n,\mathbf{k}} \frac{n_F(\epsilon_{n,\mathbf{k}}) - n_F(\epsilon_{n',\mathbf{k}+\mathbf{q}})}{\epsilon_{n',\mathbf{k}+\mathbf{q}} - \epsilon_{n,\mathbf{k}}} \times |\langle n', \mathbf{k} + \mathbf{q} | s_z | n, \mathbf{k} \rangle|^2. \quad (17)$$

As explained in the previous section, we will consider a space-isotropic susceptibility $\chi(q)$ obtained by angular averaging the true susceptibility. This leads to a function $j(q)$ depending only on the modulus of \mathbf{q} , from which real-space couplings are easily extracted.

Our main concern will be obtaining critical temperatures from MC simulations. Nevertheless, we will also compare MC calculations with the predictions of mean-field ap-

proaches. We believe this is interesting for, given the usual computer limitations of MC calculations, this comparison allows us to gauge the merits and shortcoming of standard mean-field techniques. In addition, we will show that simple considerations concerning the effect of fluctuations allow us to estimate how far the mean-field temperature is from the real one. Therefore, we devote the rest of this section to this analysis.

In the standard mean-field approach, the critical temperature can be read-off from the effective field experienced by a magnetic impurity. In our site disordered system, this can be written as follows:

$$k_B T_C^{mf} = \frac{S^2}{3} \left\langle \sum_{I \neq 0} x_i J(\mathbf{R}_I) \right\rangle = \frac{S^2}{3} x \sum_{I \neq 0} J(\mathbf{R}_I), \quad (18)$$

where the sum runs over all sites of the fcc lattice and the average is taken over disorder configuration. The latter is characterized by the random variable x_i , which marks the presence ($x_i=1$) or absence ($x_i=0$) of impurity at site i , with average $\langle x_i \rangle = x$.

The sum can be evaluated in Fourier space as follows:

$$\begin{aligned} k_B T_C^{mf} &= \frac{S^2}{3} x \left(\sum_i J(\mathbf{R}_i) - J(\mathbf{R}=0) \right) \\ &= \frac{S^2}{3} x \left(J_{pd}^2 \frac{N}{\Omega} \chi_p(\mathbf{q} \rightarrow 0) - \frac{1}{N} \sum_{\mathbf{q}} j(\mathbf{q}) \right) \\ &= k_B T_C^{vca} \left(1 - \frac{1}{N} \sum_{\mathbf{q}} \frac{\chi_p(q) e^{-q^2 a_0^2}}{\chi_p(q \rightarrow 0)} \right). \end{aligned} \quad (19)$$

Notice that the self-interaction must be explicitly removed. If it is not, one ends up with a different mean-field approximation which we have previously termed the virtual-crystal approximation T_C^{vca} . Looking at the Heisenberg Hamiltonian of Eq. (14), it is clear from a conceptual point of view that the *genuine* mean-field approximation requires this removal of the self-interaction term, even if both temperatures turn out to be similar in the physical region of parameters. It is this suppression of self-interaction that accounts for the reduction, and even the disappearance, of the critical temperature with increasing carrier concentration, owing to the oscillatory nature of the exchange coupling. While T_C^{mf} accounts for this effect, the VCA approach is blind to this oscillation, always predicting a finite transition temperature.

It is well known that mean-field approximations tend to overestimate the transition temperature due to the neglect of fluctuations. Nevertheless, the effect of the neglected fluctuations, and their influence on the transition temperature, can be estimated by means of a consistency criterion, similar in spirit to the well-known Ginsburg criterion (see any text on critical phenomena, for instance, Ref. 24), as we now explain. The mean-field approach assumes independent spins under the influence of a molecular field determined self-consistently. At $T = T_C^{mf}$, the average molecular field is zero, and so is the magnetization. Yet, even within this mean-field scenario, there are fluctuations around the zero average field. In the present case, where the interaction can extend over

large distances for small carrier concentration, this molecular field will be the sum of many random variables, therefore a Gaussian distribution is expected for it. At the critical temperature, we can write the following expression for the distribution of molecular fields along the z axis:

$$\mathcal{P}(h_{mol}) = \frac{1}{(2\pi\Delta h_{mol})^{1/2}} \exp\left(-\frac{h_{mol}^2}{2(\Delta h_{mol})^2}\right), \quad (20)$$

with a dispersion in local fields given by

$$(\Delta h_{mol})^2 = \frac{xS^2}{3} \sum_{I \neq 0} [J(\mathbf{R}_I)]^2, \quad (21)$$

where the lattice sum can be evaluated in Fourier space as

$$\sum_{I \neq 0} [J(\mathbf{R}_I)]^2 = \frac{1}{N} \sum_{\mathbf{q}} |J(\mathbf{q})|^2 - \left(\frac{1}{N} \sum_{\mathbf{q}} J(\mathbf{q}) \right)^2. \quad (22)$$

Notice that both thermal and positional disorder contribute to the expression of Eq. (21).

This means that even though the average (spontaneous) magnetization is zero at the nominal critical temperature T_C^{mf} , there will be a distribution of local magnetizations, with a dispersion given by

$$\langle m^2 \rangle_{T_C^{mf}} = \int dh_{mol} \mathcal{P}(h_{mol}) [S\tilde{\mathcal{M}}(\tilde{h}_{mol})]^2, \quad (23)$$

where

$$\tilde{\mathcal{M}}(\tilde{h}_{mol}) = \left(\frac{1}{\tanh(\tilde{h}_{mol})} - \frac{1}{\tilde{h}_{mol}} \right) \quad (24)$$

is the normalized magnetization of an isolated impurity in the presence of the (dimensionless) molecular field $\tilde{h}_{mol} = Sh_{mol}/(kT_C^{mf})$.

This provides us with a natural consistency criterion for the validity of mean-field results. We can say, for instance, that we will trust the mean-field results for temperatures $T \leq T^* < T_C^{mf}$ such that the average, spontaneous, mean field magnetization $m(T^*)$ is much larger than the “incertitude” of the magnetization at T_C^{mf} due to fluctuations (several variants of this criterion can be envisaged). To be specific, we will define a temperature T^* such that

$$[m(T^*)]^2 = \mathcal{G} \langle m^2 \rangle_{T_C^{mf}}, \quad (25)$$

where \mathcal{G} is a “large,” dimensionless parameter, and the mean-field magnetization is the well-known implicit solution of $m = S\tilde{\mathcal{M}}(3(T/T_C^{mf})(m/S))$. We have chosen the value of \mathcal{G} by looking at the simplest Heisenberg model: classical spins in a cubic lattice with nearest-neighbor couplings. In this simpler *reference* model, the value of \mathcal{G} is obtained by demanding that if the previous scheme is applied, the T^* so obtained coincides with the MC determined temperature for that model.²⁵ The actual value is around $\mathcal{G} = 8.3$. Irrespective of the precise numerical value of the coefficient \mathcal{G} , it is clear that the T^* so obtained is a direct measure of the effect of

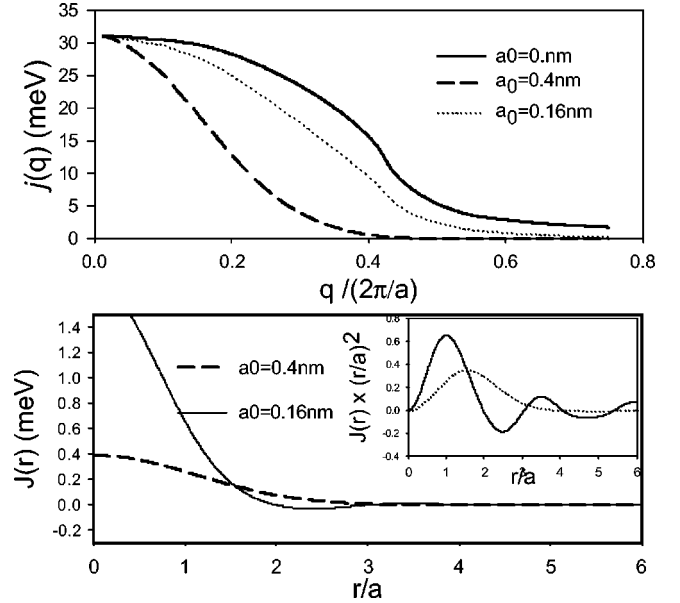


FIG. 4. Top panel: Fourier transform of the interaction energy as function of q for a two-band model with $m^* = 0.5$, $p = 0.44 \text{ nm}^{-3}$, $J_{pd} = 0.06 \text{ eV nm}^3$. Bottom panel: Real-space exchange coupling as function of r for a two-band model with the same parameters.

fluctuations and, therefore, of the corrections to the mean-field temperatures. We will term this T^* the fluctuations-corrected critical temperature.

V. RESULTS: EXCHANGE INTERACTIONS, CURIE TEMPERATURES, AND MAGNETIZATION

A. Two-band model

As a first example, we apply our method to the simplest case of a two-band model. In this model, the wave functions are plane waves of momentum \mathbf{k} with a dispersion relation $\hbar^2 k^2 / (2m^*)$, m^* being the average effective mass of the holes. In Fig. 4 (top panel) we show the Fourier transform of the exchange interaction for $J_{pd} = 0.06 \text{ eV nm}^3$, $m^* = 0.5$, and different values of a_0 . For $a_0 = 0$, $j(q)$ is proportional to the paramagnetic susceptibility, which coincides with the Lindhard function²⁶ and exhibits the well-known anomaly in the second derivative at $2k_F$. For $a_0 = 0$, the paramagnetic susceptibility of the carriers decays very slowly as a function of q , and the value of the coupling $j(q)$ is significant even for values of q near the zone boundary $2\pi/a$. This result is unlikely as the effective-mass approximation and the $\mathbf{k} \cdot \mathbf{p}$ method are just applicable for describing the semiconductor band structure near the center of the Brillouin zone. Fortunately, this problem is solved when we introduce a finite spatial extent a_0 for the coupling between Mn and carriers. In this paper we perform calculations for $a_0 = 1.6 \text{ Å}$ and 4 Å . For $a_0 = 1.6 \text{ Å}$, the interaction decays rather slowly in reciprocal space, although its value at the zone boundary is practically zero, Fig. 4. For $a_0 = 4 \text{ Å}$, the interaction decays rather fast in reciprocal space, being nearly zero at half the Brillouin zone. The value $a_0 = 4 \text{ Å}$ corresponds to the first neighbors distance in the fcc lattice with $a = 5.66 \text{ Å}$.

In Fig. 4 (bottom panel) we show the real-space coupling constant as a function of r/a for the same parameters. For $a_0=0$, this is nothing but the RKKY interaction:

$$J_{\text{two-band}}(r) \sim \frac{2k_F r \cos(2k_F r) - \sin(2k_F r)}{(2k_F r)^4}. \quad (26)$$

This function decays as r^3 and oscillates in sign with the distance. This oscillatory behavior is a signature of the $2k_F$ anomaly that occurs in the paramagnetic susceptibility. For finite values of a_0 , the $2k_F$ anomaly in $j(q)$ is softened, and the oscillatory behavior of the real-space coupling $J(r)$ is damped, although for $a_0=1.6 \text{ \AA}$ it remains notable. It is important to remark the rather long-range character of the interaction between Mn spins. Even for the case of $a_0=4 \text{ \AA}$, the coupling is significant up to distances three times larger than the fcc lattice parameter. Note that in the fcc lattice, the number of neighbors for a distance cutoff of $3a$ is around 500. Therefore, in the Heisenberg Hamiltonian [Eq. (14)], the number of neighbors to be taken into account is of the order of $x \times 500$, at least.

Once the real-space exchange-coupling constants are known, we perform classical MC simulations on the orientation of the Mn spins. We use a fcc supercell of volume $N^3(a^3/4)$ with $N=30$, including more than 1200 Mn ions. For this system size, we have checked that the results are free of size effects, and that the disorder in the Mn ion positions is self-averaged. Due to the long-range character of the interaction, we have to include the interaction of each Mn spin with its first 150 neighbors in the MC simulation. This corresponds to a real-space cutoff bigger than $5a$. For distances larger than $5a$, the interaction can be neglected, as shown in Fig. 4.

The most notable result is the absence of a finite Curie temperature in the MC simulations for small values of a_0 and large values of the hole density. We have checked the absence of spontaneous magnetization for $a_0=1.6$, and carrier densities above $p=0.44 \text{ nm}^{-3}$. For a density $p=0.22 \text{ nm}^{-3}$, we obtain a Curie temperature of 14 K, considerably smaller than the mean-field value. It is interesting to realize that the fluctuation analysis described previously fits nicely with these MC results. In Fig. 5(a), we plot the predictions of the mean-field treatments, along with the expected corrections from the neglect of fluctuations. We see that, for $p \sim 0.44 \text{ nm}^{-3}$, the fluctuations have grown to the point that no finite temperature exists, meeting the consistency criterion described in Eq. (25), in agreement with the absence of magnetization observed in MC simulations. Notice that for lower carrier concentration, a finite magnetization reemerges. In fact, the mean-field temperatures T_C^{mf} , T_C^{vca} , and the fluctuations-corrected temperature T^* merge in the very low density limit, as shown in Fig. 5. This is not surprising, for a vanishing k_F implies long-ranged interactions where the neglect of fluctuations becomes increasingly irrelevant, leading to the asymptotic correctness of mean-field results.

Increasing the spatial extension of the coupling between impurities and carriers to $a_0=4 \text{ \AA}$, the RKKY oscillations

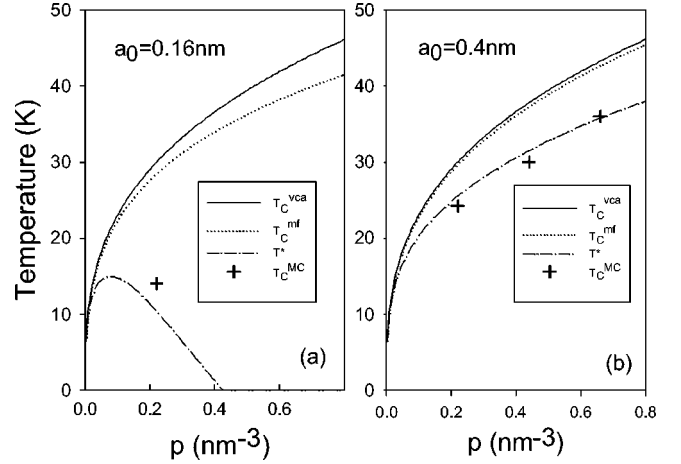


FIG. 5. Curie temperatures (Monte Carlo, mean field, and fluctuations corrected) for the two-band model with $m^*=0.5$ as a function of the hole density for $x=0.05$, for two values of a_0 .

are damped and a low-temperature ferromagnetic GS appears in MC calculations. In Fig. 5(b), we plot the MC Curie temperatures for different hole densities, along with the fluctuations-corrected T^* and the mean-field results, both with and without self-interaction corrections. The observed MC temperatures are consistent with the fluctuations-corrected T^* . From this analysis, it is clear that Curie temperatures approach the mean-field results with increasing nonlocality (larger values of a_0) in the coupling between impurities and carriers.

B. $\mathbf{k} \cdot \mathbf{p}$ model

The $\mathbf{k} \cdot \mathbf{p}$ model describes the valence band of the semiconductors in a realistic way. The most characteristic features of the GaAs valence bands are the anisotropy in reciprocal space and the strong coupling between the heavy- and light-hole bands. These effects substantially alter the constant energy surfaces of the holes states, which become nonspherical, with a warped shape. The lack of a well-defined modulus of the Fermi wave vector softens the $2k_F$ anomaly in the average paramagnetic susceptibility as a function of q . This is clear in Fig. 6 (top panel), where we plot the Fourier transform of the interaction energy for the same parameters as in Fig. 4, for $a_0=1.6 \text{ \AA}$ and $a_0=4 \text{ \AA}$. In the bottom panel of Fig. 6, we plot the real-space energy coupling $J(r)$. It decays almost continuously to zero with a very weak oscillation, as expected from the absence of strong anomalies in $j(q)$. As in the two-band model, we obtain that the interaction between Mn ions extends several lattice sites, and the quantity of merit, $J(r)r^2$ (see inset of Fig. 6), has a maximum near $r=2a$, for both values of $a_0=1.6 \text{ \AA}$ and $a_0=4 \text{ \AA}$.

We have performed MC simulation with the coupling constants shown in Fig. 6 and a concentration of 5% for Mn ions. The details of the simulation are the same as in the two-band case. Representative results for the Mn spin polarization as a function of temperature are shown in Fig. 7. In Fig. 8, we exhibit the MC Curie temperatures along with the mean-field and fluctuation-corrected results. Comparing with

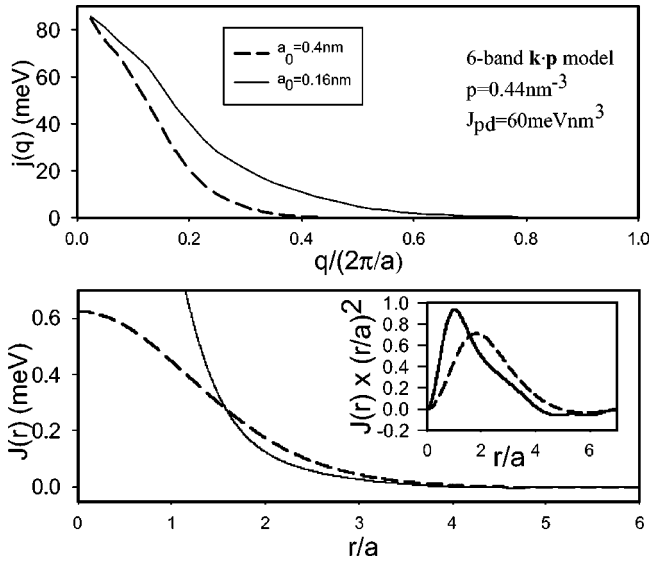


FIG. 6. Top panel: Fourier transform of the interaction energy as function of q for the $\mathbf{k} \cdot \mathbf{p}$ model. Bottom panel: Real-space coupling as function of r .

the corresponding results for the two-band case, the six-band model shows an overall increase of transition temperatures. In addition, the MC temperatures are closer to the mean-field results than in the two-band case, for the same parameters. It is interesting to note that, again, the fluctuation-corrected temperature T^* offers a fair estimation of the MC temperature. In any case, the combined effect of thermal and disorder fluctuations is much less severe than in the two-band case. This is evident, for instance, in the curves for $a_0=4\text{Å}$, where the VCA transition temperature T_C^{vca} already provides a good estimation of the MC T_C . This is consistent with the

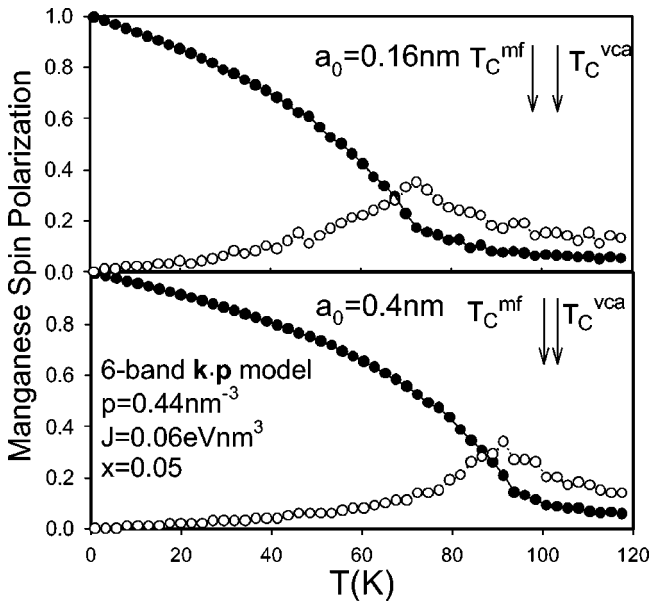


FIG. 7. Closed dots represent the temperature dependence of the Mn spin polarization as obtained from MC simulations for the $\mathbf{k} \cdot \mathbf{p}$ model. Open dots correspond to Mn spin polarization fluctuations, which help to estimate the value of the Curie temperature.

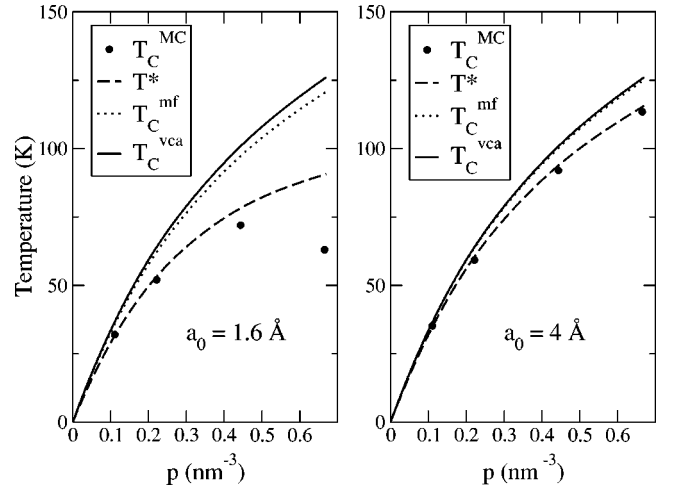


FIG. 8. $\mathbf{k} \cdot \mathbf{p}$ model Curie temperatures from MC calculations as a function of hole density, compared with results of mean-field temperatures T_C^{vca} , T_C^{mf} , and the fluctuations-corrected critical temperature T^* , for Mn concentration $x=0.05$.

fact that interactions in this six-band case, while extending several lattice sites, do not manifest the violent sign oscillations present in the two-band calculation. As in the two-band calculation, mean-field and exact (MC) temperatures tend to merge at low carrier density, as expected from the increasing range of the exchange coupling between Mn ions. Similarly, increasing the spatial extent of the interaction between Mn ions and carriers (a_0) softens the effect of fluctuations, leading to a better agreement between mean-field and MC temperatures.

VI. COLLECTIVE EXCITATIONS OF THE $T=0$ GROUND STATE

In this section, we study the low-energy collective magnetic excitations of DMS at zero temperature. We assume that at $T=0$, Mn spins are fully polarized, and the spin polarization of the carriers, ξ , is obtained by solving the carriers Schrodinger equation in the presence of the uniform magnetic field created by the Mn ions, $SJ_{pd}c$. The low-energy collective magnetic excitations of the system are obtained from the Heisenberg Hamiltonian

$$H_\xi = E_{KE}(\xi) - \sum_{I,J} J_\xi(\mathbf{R}_{IJ}) \mathbf{S}_I \cdot \mathbf{S}_J, \quad (27)$$

where $E_{KE}(\xi)$ is the kinetic energy of the carriers evaluated at the hole spin polarization ξ . This Hamiltonian describes small oscillations of the Mn spins from the fully polarized state, which we choose to point in the z direction. The Fourier transform of the coupling constants $J_\xi(\mathbf{R}_{IJ})$ is proportional to the transverse response function of the polarized hole gas $\chi^\perp(q, \xi)$:

$$j_\xi(q) = J_{pd}^2 \frac{N}{\Omega} \chi^\perp(q, \xi) e^{-q^2 a_0^2}. \quad (28)$$

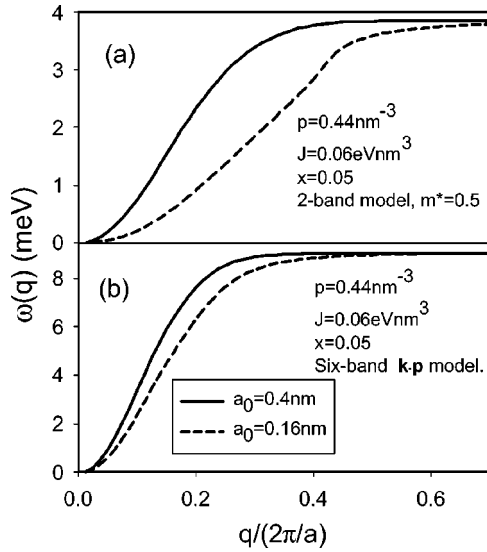


FIG. 9. Spin-wave dispersion, obtained in the virtual-crystal approximation, for the two-band model (a) and for the $\mathbf{k} \cdot \mathbf{p}$ model (b). The carriers spin polarization is $\xi = 0.69$ in both figures.

In writing Eqs. (27) and (28) we assume, as we have justified in preceding sections, that the Mn interaction energy can be expressed as a sum of Mn spin-pair interactions, which only depends on the relative angle formed by the Mn spins and on the distance separating them. We have also neglected the magnetic anisotropy energy that we know is very small.^{6,7}

The low-energy collective excitations are obtained by solving the equation of motion of the Mn spins:

$$-i\hbar \frac{\partial S_I^-}{\partial t} = [H_\xi, S_I^-] = - \sum_j J_\xi(\mathbf{R}_{I,j}) (S_I^z S_j^- - S_j^z S_I^-). \quad (29)$$

Near $T=0$, the Mn spins are fully polarized, we replace S^z by S and the equations may be linearized.

A. Spin waves in the VCA

In the VCA, all sites are equivalent and, in Eq. (29), the sum over the Mn positions is replaced by a sum over all lattice positions times the Mn concentration x . In this approximation the collective excitations are spin waves with momentum \mathbf{q} and dispersion relation

$$\omega(\mathbf{q}) = xS[J_\xi(q=0) - J_\xi(q)]. \quad (30)$$

In Fig. 9 we plot the spin-wave dispersion for the two-band model and for the six-band $\mathbf{k} \cdot \mathbf{p}$ model with typical values of the parameters and for both $a_0 = 4 \text{ \AA}$ and $a_0 = 1.6 \text{ \AA}$. The spin waves are gapless as the model Hamiltonian (27) is invariant under rotations. At small values of the wave vector, the spin waves disperse quadratically and the expression $\omega(q) = \rho_s q^2 / (2\pi/a)$ defines the spin stiffness ρ_s . The spin waves are harder in the six-band $\mathbf{k} \cdot \mathbf{p}$ model ($\rho_s = 242 \text{ meV}$ and 370 meV , for $a_0 = 1.6 \text{ \AA}$ and $a_0 = 4 \text{ \AA}$, respectively) than in the two-band model ($\rho_s = 18 \text{ meV}$ and 76 meV , for $a_0 = 1.6 \text{ \AA}$ and $a_0 = 4 \text{ \AA}$, respectively). This is consistent with the fact that the Curie temperature is larger in the $\mathbf{k} \cdot \mathbf{p}$

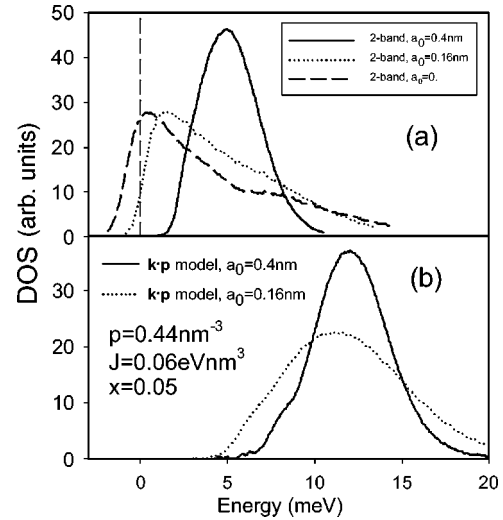


FIG. 10. Density of states for low-energy excitations in the two-band model and in the $\mathbf{k} \cdot \mathbf{p}$ model, obtained from the equation of motion method. The DOS is averaged over different disorder realizations. The parameters used are the same as in Fig. 9.

model than in the two-band model. Also, we find that the stiffness increases as a_0 increases. These numerical results for the stiffness agree with those obtained by König *et al.* using a formalism that treats the Mn spins as noninteracting bosons.²⁷

B. Effect of the disorder

In this section we analyze the effect of the disorder on collective magnetic excitations of the $T=0$ ferromagnetic ground state. To this end, we diagonalize the equations of motion, Eq. (29), for different disorder realizations. We place the Mn ions randomly on a fcc lattice, and consider the interaction of each Mn with all its neighbors within a distance shorter than six lattice units. We consider systems with more than, typically, 500 Mn spins, and use periodic boundary conditions. In the presence of disorder, the collective excitations cannot be characterized by a wave vector and we, therefore, analyze their density of states (DOS). In Fig. 10 we plot the DOS of the collective excitations for the two-band model and for the six-band $\mathbf{k} \cdot \mathbf{p}$ model, for different values of a_0 . The DOS is obtained by averaging over different disorder realizations. For every disorder realization, we always obtain a zero energy mode that corresponds to a uniform rotation of all the Mn spins. This Goldstone mode reflects the symmetry of the Hamiltonian Eq. (27). In Fig. 10(a) we see that in the two-band model and for short spatial extension of the spin interaction, there are collective excitations with *negative* energy. This implies that the fully polarized GS is unstable. This instability is due to the long-range oscillations of the interaction between the Mn spins. For $a_0 = 4 \text{ \AA}$ these oscillations are damped and the fully polarized ferromagnetic GS is stable.

In Fig. 10(b), we plot the DOS for the six-band $\mathbf{k} \cdot \mathbf{p}$ model. Our results show that the fully polarized ferromagnetic GS is stable for any value of a_0 at the density of carriers studied. This stability is the result of the Fermi surface

warping produced by the heavy-hole light-hole mixing in the $\mathbf{k}\cdot\mathbf{p}$ Hamiltonian. The holes do not have a well-defined $2k_F$ anomaly in the response functions.

This stability analysis obtained from the study of the ferromagnetic low-energy excitations is in agreement with the results presented in the preceding section. Note, however, that only the paramagnetic spin susceptibility enters the interaction between Mn spins for the calculated Curie temperatures.

Recently Schlienman *et al.*^{15,16} have computed the $T=0$ response function of DMS and have suggested that, in general, the GS of DMS should be noncollinear. In their calculations they use a two-band model, and the instability is the same that we find in Fig. 10(a). From our calculations we conclude that the instabilities found in Refs. 15,16 are just due to the model considered, and disappear when a more realistic band-structure model is used.

VII. CONCLUSIONS

We have introduced a Heisenberg-like Hamiltonian, Eq. (14), for describing the magnetic properties of GaMnAs. This model just requires the positions and the orientations of the Mn spins. The use of this model is justified because (i) the energy of the system can be written as a sum of pair interactions, (ii) the interaction between two Mn spins is well described by their scalar product, and (iii) the coupling constants of the Heisenberg model depend basically on the distance between Mn spins and can be evaluated perturbatively.

As the electronic properties of the host semiconductor are integrated into the coupling constants of the Heisenberg Hamiltonian, it is possible to perform MC simulations in systems with a large number of Mn spins, and so to obtain the Curie temperature of the DMS. We have compared the Monte Carlo, mean-field, and a fluctuation-corrected critical temperatures for different band-structure models and for different values of the exchange-coupling spatial extension a_0 . The fluctuation effects are important for large hole densities, being more relevant for smaller values of a_0 .

In the two-band model, the existence of a well-defined $2k_F$ anomaly produces a long-range interaction between Mn spins that oscillates in sign with the distance. The fluctuations are magnified by these oscillations which can lead to

the disappearance of the ferromagnetic state from moderate to large values of the hole density. We find that for a_0 smaller than 1.6 Å and hole densities larger than 0.44 nm^{-3} , there is no finite Curie temperature. When the value of a_0 increases, the interaction oscillations are damped and a finite Curie temperature appears.

In the $\mathbf{k}\cdot\mathbf{p}$ model, the warping of the Fermi surface softens the $2k_F$ anomaly in the response function and the real-space interaction oscillations are almost suppressed. Therefore, the effect of fluctuations is weaker than in the two-band model. We find that for $a_0=4\text{ Å}$, the fluctuations effect reduces the Curie temperature by no more than 10%. For smaller values of a_0 , the effect of fluctuations is more severe, with Curie temperatures reduced by almost 50%, for $p=0.66\text{ nm}^{-3}$. Nevertheless, we believe that a value of a_0 close to 4 Å is appropriated, as it corresponds to the first neighbors distance in the fcc lattice. This is the minimum separation between the Mn-*d* orbitals and the GaAs-*p* orbitals that form the hole band of the semiconductor.

Finally, we have studied our model in the zero-temperature limit. We have computed the low-energy collective magnetic excitations of the $T=0$ ferromagnetic ground state. In agreement with the Monte Carlo results, we find that for the two-band model and moderate to large hole densities, the ferromagnetic ground state is no longer stable. However, when a more realistic six-band $\mathbf{k}\cdot\mathbf{p}$ model is used, the stability of the fully polarized ferromagnetic ground state is recovered.

From our calculation, we conclude that the use of a realistic electronic structure for describing the properties of the host semiconductor produces a hole mediated interaction between Mn spins with virtually no sign oscillations. Therefore, we believe that the observed lack of magnetization saturation in DMS should be related with extrinsic effects rather than with intrinsic frustration in the system.

ACKNOWLEDGMENTS

We are grateful to J. Fernández Rossier and A. H. MacDonald for helpful discussions. Financial support is acknowledged from Grant Nos. MAT2002-04429-C03-01 and MAT2002-04095-C02-01 (MCyT, Spain), and Fundación Ramón Areces.

¹F. Matsukura, H. Ohno, A. Shen, and Y. Sugawara, Phys. Rev. B **57**, R2037 (1998).

²H. Ohno, Science **281**, 951 (1998).

³H. Ohno and F. Matsukura, Solid State Commun. **117**, 179 (2001).

⁴T. Dietl, *Diluted Magnetic Semiconductors, Handbook of Semiconductors* Vol. 3B (North-Holland, New York, 1994).

⁵F.D. Chiba, K. Takamura, and K. Ohno, Appl. Phys. Lett. **82**, 3020 (2003).

⁶T. Dietl, H. Ohno, F. Matsukura, J. Cibert, and D. Ferrand, Science **287**, 1019 (2000).

⁷T. Jungwirth, W.A. Atkinson, B.H. Lee, and A.H. MacDonald,

Phys. Rev. B **59**, 9818 (1999).

⁸Along this paper we take $g\mu_B=1$ in the definition of the magnetic susceptibility.

⁹S.J. Potashnik, K.C. Ku, R. Mahendiran, S.H. Chun, R.F. Wang, N. Samarth, and P. Schiffer, Phys. Rev. B **66**, 012408 (2002).

¹⁰K.W. Edmonds, K.Y. Wang, R.P. Campion, A.C. Neumann, N.R.S. Farley, B.L. Gallagher, and C.T. Foxon, Appl. Phys. Lett. **81**, 4991 (2002).

¹¹J. Schliemann, J. König, and A.H. MacDonald, Phys. Rev. B **64**, 165201 (2001).

¹²G. Alvarez, M. Mayr, and E. Dagotto, Phys. Rev. Lett. **89**, 277202 (2002).

- ¹³M.J. Calderón, G. Gómez-Santos, and L. Brey, Phys. Rev. B **66**, 075218 (2002).
- ¹⁴M. Berciu and R.N. Bhatt, Phys. Rev. Lett. **87**, 107203 (2000).
- ¹⁵J. Schliemann and A.H. MacDonald, Phys. Rev. Lett. **88**, 137201 (2002).
- ¹⁶J. Schliemann, Phys. Rev. B **67**, 045202 (2003).
- ¹⁷G. Zaránd and B. Jankó, Phys. Rev. Lett. **89**, 047201 (2002).
- ¹⁸D.J. Priour, Jr., E.H. Hwang, and S. Das Sarma, cond-mat/0305413 (unpublished).
- ¹⁹J. Okabayashi, A. Kimura, O. Rader, T. Mizokawa, A. Fujimori, T. Hayashi, and M. Tanaka, Phys. Rev. B **58**, R4211 (1998).
- ²⁰M. Abolfath, T. Jungwirth, J. Brum, and A.H. MacDonald, Phys. Rev. B **63**, 054418 (2001).
- ²¹C. Timm, F. Schafer, and F. von Oppen, Phys. Rev. Lett. **89**, 137201 (2002).
- ²²P.Y. Yu and M. Cardona, *Fundamentals of Semiconductors* (Springer-Verlag, New York, 1996).
- ²³A. Baldereschi and N.O. Lipari, Phys. Rev. B **8**, 2697 (1973).
- ²⁴J. Cardy, *Scaling and Renormalization in Statistical Physics* (Cambridge University Press, Cambridge, 1996).
- ²⁵M.H. Lau and C. Dasgupta, Phys. Rev. B **39**, 7212 (1989).
- ²⁶D. Pines and P. Nozieres, *The Theory of Quantum Liquids* (W.A. Benjamin, Inc., New York, 1966).
- ²⁷J. König, H.H. Lin, and A.H. MacDonald, Phys. Rev. Lett. **84**, 5628 (2000).